



Mother Optimization Algorithm for Solar PV System under Partial Shading

Massara Glaa Yahya ^{1,a}

¹ Department of Civil Engineering, Al-Nahrain University, Baghdad, Iraq

^a Corresponding author's email: meserra.gelaa@nahrainuniv.edu.iq (<https://orcid.org/0000-0002-1507-6126>)

Article info

Received 24 August 2024
Revised 22 November 2024
Accepted 3 December 2024
Available online 1 January 2025

Keywords: *Mother Optimization Algorithm (MOA); Partial Shading Condition (PSC); Maximum Power Point (MPPT); photovoltaic (PV).*

Abstract.

This work investigates the combined use of the traditional Perturb and Observe (P&O) algorithm with the Mother Optimization Algorithm (MOA) for tracking the Global Maximum Power Point (GMPP) and a DC-DC boost converter. The results indicate that the MOA algorithm captures GMPP with 98% efficiency in MATLAB Simulink running under partial shading condition (PSC), while the P&O approach fails to capture GMPP.

1. Introduction

Use Photovoltaic (PV) systems are ubiquitous in modern life due to the numerous benefits of solar energy, including its decreased cost and increased usability over extended periods of time. Nevertheless, PV systems' limited energy efficiency and relatively short lifespans pose significant challenges in real-world scenarios. Partial shadows are the primary cause of this, as they result in PV modules receiving variable irradiance. Thus, there are several peaks on the P-V characteristic curve. The GP is one of several local peaks (LP).

[1]. When the quantity of sunshine is constant, traditional methods for determining when solar systems produce the greatest amount of power can be effective. By connecting bypass diodes, a solar system operating in the partial shade can lessen the effect of hot spots on its output. Among these techniques are the widely utilized perturb and observe (P&O) [2], [3], and incremental conductance (IC) [4] algorithms. They are obvious to recognize and simple to put into practice. Nevertheless, they are unstable near the Maximum Power Point (MPP) and are unable to adapt to changes in their surroundings. Factors Influencing Partial Overcasting The power-voltage characteristic curve will exhibit distinct local maximum points in partial

shading condition (PSC). Multiple peaks on the photovoltaic (PV) characteristic curve add considerable complexity to power extraction. To achieve maximum power and optimize efficiency, a control system must be developed that can differentiate between local and global maxima [5]. The Global Maximum Power Point (GMPP) can be consistently identified under varying atmospheric conditions, irrespective of the uniformity of solar irradiation. Various global MPP search techniques have been specifically designed to address the challenges posed by partial shading. Many of these techniques have drawbacks, such as being costly, difficult to apply, or necessitating measurements on numerous factors [6].

Numerous methods for finding MPPs have been developed in research to compute the global MPP in certain shadow scenarios. A few publications describing attempts to address this kind of challenge have been published. In addition, many of these methods present drawbacks, such as complexity, difficulty in development, high costs, and the requirement for extensive tracked data. Oulcaid et al. [7] built a solar array point tracking system using an Artificial Neural Network (ANN) using three feed-forward layers based on polar information. However, the results of this method were limited in a few ways,

including the excessive complexity of the control scheme and the large number of computations.

In this paper, the mother optimization algorithm MOA has been used to achieve the maximum point tracking under partial shading, and then compared it with the conventional MPPTs especially P/O algorithm.

The Perturb and observe algorithm is discussed in Section 3, whereas Section 2 covers the simulation of PV and MPPT. The Mother optimization algorithm is discussed in Section 4. Section 5 addresses the Partial Shading Principle. The operation of the DC-DC boost converter is covered in Section 6, while Section 7 focuses on the modeling of the circuit diagram. Section 8 presents the results and analysis of the simulation, and Section 9 provides the conclusion of the paper.

2. Modelling of Photovoltaic and Maximum Power Point Tracking Systems

The photovoltaic arrays in photovoltaic systems convert the sun's rays into electricity. Photovoltaic arrays are often utilized, never run out of power, and are simple to maintain because of their cleanliness. Power converters are necessary for photovoltaic systems in order to transport power between the sunlight generated by the panels to the load. A photovoltaic cell can be considered a non-linear circuit containing a diode and a current source, as depicted in Figure 1. During periods of inactivity, the diode prevents any reverse current from flowing into the panel from energy storage devices [8]. The practical model of a PV cell also incorporates the internal resistances, R_s (series) and R_p (parallel), which demonstrate a low series resistance and a high shunt resistance. Calculations indicate that these resistance values have minimal effect on the overall performance of the cells [8, 9].

$$I = I_{PV,cell} - I_o [\exp(V + R_s I / N_t a) - 1] \quad (1)$$

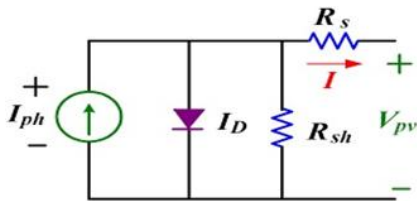


Figure 1. A photovoltaic cell's equivalent circuits

$$V_t = N_s k T/q \quad (2)$$

Where:

V photovoltaic systems output voltages.

q electron charge “ $1.60217646 \times 10^{-19} \text{ C}$ ”.

I : The photovoltaic system's output current.

V_t : The array of series-connected N_s cells' thermal voltage.

k : The Boltzmann constant ($1.3806503 \times 10^{-23} \text{ J K}^{-1}$).

a : The ideality constant of diodes.”

T : The Kelvin value of the p-n junction.

The light generated current of the photovoltaic cell is denoted by $I_{PV,cell}$ in the following equation [8]:

$$I_{PV,cell} = (I_{PV,n} + K_i \Delta T) G/G_n \quad (3)$$

$$\Delta T = T - T_n \quad (4)$$

Where:

$I_{PV,n}$: The current produced by light at 25°C and 1000 W m^{-2} .

T : The real temp. expressed (K).

T_n : The Kelvin unit of both the nominal and actual temperature.

G : The amount of solar energy that the PV surface receives.

G_n : The stated amount of solar radiation.”

The relationship between the diode's saturation current, denoted by I_o , and its temperature dependency can be expressed as follows [20]:

$$I_o = [(I_{sc,n} + K_i \Delta T)/\exp(V_{oc,n} + K_v \Delta T/aV_t) - I] \quad (5)$$

Where:

K_i : The temperature/current short-circuit coefficient.

K_v : The voltage/temperature coefficient in open circuit.

$V_{oc,n}$: The voltage of the open circuit when it is nominal.

$I_{sc,n}$: The current in the short circuit under nominal conditions.

The PV system must produce its maximum amount of power. The maximum power point method should be used by designers of photovoltaic devices since temperature and sunlight irradiation affect PV array output power. Because SPV systems aren't very efficient, there are a lot of ways to make them more so that production and usage are both balanced. The combination of MPPT and its monitoring method maximizes the power output from a variable source. Through the use of a boost converter, the MPPT controller can deliver the greatest amount of power from the array to the load. Options for MPPT control include P&O, PSO, FLC, and a search based on the Fibonacci numbers. Mother Optimization Algorithm (MOA) is used to implement MPPT control in the study. According to Table 1, the following are the specifications

of a simulated solar power system (Motech Americas IM72D3-330).

Table 1. A PV module's (Motech Americas IM72D3-330) simulation parameters

Model	Clearline PV
Max. Power (P_{max})	330W
Voltage at Max. Power (V_{mp})	37.66V
Current at Max. Power (I_{mp})	8.76A
Short Circuit Current (I_{sc})	9.27A
Open Circuit Voltage (V_{oc})	45.73V
Number of series cells N_s	2
Number of cells (N)	72
Number of parallel cells N_p	1

3. Perturb / observe algorithm

Commonly employed in photovoltaic (PV) systems to run DC/DC converters at a regulated duty cycle to maintain MPP. The benefits of this approach include its simplicity, affordability, and ease of implementation. P&O's fundamental idea is to slightly alter the output voltage and then track the change in output power as a result. This method's primary flaws include erroneous tracking under PSC and oscillation around MPP. The P&O method's methodology is shown in Fig. 2[10].

4. Mother optimization algorithm

The mother algorithm for optimization (MOA) with its mathematical model will be introduced in this part. The goal of this part is to provide a thorough introduction to MOA and the underlying mathematical foundation. Through examining the algorithm's specifics and mathematical formulation, readers will have a deeper understanding of the ideas and the inner workings of MOA.

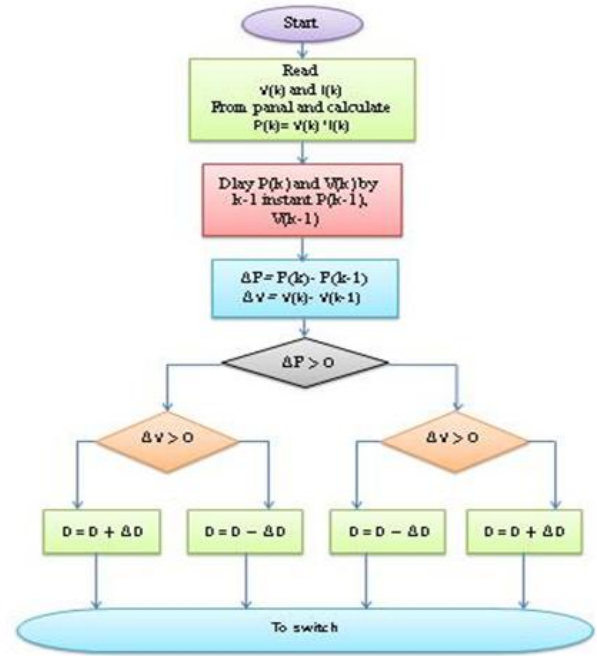


Figure 2. The P&O method algorithm

The home is unquestionably the first educational institution in society, and a mother's role as an educator is crucial while raising children. A mother imparts to her children valuable life lessons and life experiences, and they grow as a result of her guidance [11], [12]. The three processes of educating, advising, and rearing are thought to be among the most important forms of connection between a mother and her child. As a result, the proposed MOA mimics compassionate and instructive behaviors computationally.

The MOA method uses an iterative process to tackle optimization problems. The population of the algorithm is made up of potential solutions that are shown as vectors in the issue space. Eq. (6) models the population as a matrix, while Eq. (7) initializes the population at the beginning of the optimization procedure. The population's collective search power is harnessed to find the best answer; every member of the population selects decision variable values according to where it is located inside the problem search space [13].

$$X = \begin{bmatrix} X_1 \\ \vdots \\ X_i \\ \vdots \\ X_N \end{bmatrix}_{N \times m} = \begin{bmatrix} x_{1,1} & \cdots & x_{1,j} & \cdots & x_{1,m} \\ \vdots & \ddots & \vdots & \ddots & \vdots \\ x_{i,1} & \cdots & x_{i,j} & \cdots & x_{i,m} \\ \vdots & \ddots & \vdots & \ddots & \vdots \\ x_{N,1} & \cdots & x_{N,j} & \cdots & x_{N,m} \end{bmatrix}_{N \times m}, \quad (6)$$

$$“x_{i,j} = lbj + rand(0, 1) \cdot ubj - lbj-, i = 1, 2, \dots, N, j = 1, 2, \dots, m,” \quad (7)$$

Where \mathbf{X} is the suggested MOA's population matrix.

, N is the total population, m is the number of factors used to make decisions,

X_i is equal to the product of all the integers from 1 to m , where j is the index from 1 to m followed by x_i , m is the i^{th} possible answer, with $x_{i,j}$ being the j^{th} variable, and the random number generator from the interval $[0, 1]$ is the function $\text{rand}(0, 1)$. lb_j and ub_j stand for the lower and upper bounds of the j^{th} decision variable, respectively.

It is possible to ascertain the goal function of the challenge by making use of the values that every individual in the MOA population suggests for the decision variables, In addition, each individual in the population offers a potential answer to the problem that is being optimized. Eq. (8) may find employment to mathematically describe the numerical results of the objective function as a vector.

$$F = \begin{bmatrix} F_1 \\ \vdots \\ F_i \\ \vdots \\ F_N \end{bmatrix}_{N \times 1} = \begin{bmatrix} F(X_1) \\ \vdots \\ F(X_i) \\ \vdots \\ F(X_N) \end{bmatrix}_{N \times 1}, \quad (8)$$

The results of the objective function are included within the vector F , and the end result for the objective function for the i^{th} possible solution is represented by the symbol F_i . On the basis of the values of the objective function, an indicator of the level of quality of the responses that were produced by each member of the population is provided. Determining the optimal and minimum values for the objective function, respectively, the best and worst members of the population can be determined. Every iteration involves updating the placements of population members, and this also requires updating the best population member. Ultimately, the most proficient member of the population resolves the issue following the algorithm's iterations. The mathematical modeling results indicate that of the connection between a mothers caring for children a topic that will be covered in more detail Afterwards, the MOA design updates the algorithm population in three phases.

Education (exploration phase) Children's education serves as an inspiration for the initial population update step, dubbed "Education," in the suggested MOA strategy. The goal is to enhance global search and exploration capabilities through a significant repositioning of population members. In the MOA design, the mother is regarded as the most intelligent member of the population, with the education phase modeled after her behavior as a

teacher. During this phase, a new position for each member is generated using Eq. (9). If the new position leads to an improved objective function value, the previous position is replaced by the new one, as described by Eq. (10).

$$x_{i,j}^{P1} = x_{i,j} + \text{rand}(0, 1) \cdot (M_j - \text{rand}(2) \cdot x_{i,j}), \quad (9)$$

$$X_i = \begin{cases} X_i^{P1}, & F_i^{P1} \leq F_i, \\ X_i, & \text{else,} \end{cases}$$

Let M_j represent the j^{th} dimension of the mother's position, with $x_{i,j}$ indicating the j^{th} dimension of the i^{th} population member's position. The updated position of the i^{th} population member, determined during the initial phase of the MOA, is denoted by X_i , X_i^{P1} . The j^{th} dimension of the population is represented by $x_{i,j}^{P1}$, with its corresponding objective function value given by F_i^{P1} . The function $\text{rand}(0, 1)$ produces a random number uniformly distributed between 0 and 1, while $\text{rand}(2)$ generates a uniformly random integer from the set $\{1, 2\}$.

2. Exploration Phase

Investigating one of the primary duties of a mother as a parent is to counsel her children and to avoid misbehavior.

Using the mother's suggestions for the children, the second stage of the MOA's population update is created. The location of the population members is significantly altered during the exploration phase, which enhances the MOA's ability to search and explore globally. A population member's location in relation to different population members that's goal function values have greater values than their own is considered aberrant behavior that should be avoided, according to MOA design. Equation (11) is used to compare the objective function value in order to identify the set of poor behavior, BB_i , for each member. For each X_i , a member is randomly chosen from the set of unwanted behaviors, BB_i . In order to prevent the child from acting inappropriately, to begin, we use Eq. to generate unique positions for all members.

(12). Eq. (13) then substitutes this new position for the prior position of the relevant member if it increases the objective function value.

$$BB_i = \{X_k, F_k > F_i \wedge k \in \{1, 2, \dots, N\}\}, \quad \text{where } i = 1, 2, \dots, N, \quad (11)$$

$$x_{i,j}^{P2} = x_{i,j} + \text{rand}(0, 1) \cdot (x_{i,j} - \text{rand}(2) \cdot SBB_{i,j}), \quad (12)$$

$$X_i = \begin{cases} X_i^{P2}, & F_i^{P2} \leq F_i; \\ X_i, & \text{else,} \end{cases} \quad (13)$$

In this scenario, SBB_i represents the selected bad behavior for the i^{th} population member, with $SBB_{i,j}$ indicating its j^{th} dimension. BB_i denotes the set of undesirable behaviors for the i^{th} population member. The updated position for the i^{th} population member, as determined in the second phase of the MOA, is labeled as X_i^{P2} , with its j^{th} dimension represented by $x_{i,j}^{P2}$. The value of the objective function for this updated position is denoted as F_i^{P2} . The function $\text{rand}(0, 1)$ generates a random number uniformly between 0 and 1, whereas $\text{rand}(2)$ generates a random integer uniformly between 1 and 2. In this case, BB_i refers to the set of undesirable behaviors for the i^{th} population member, while SBB_i represents the chosen bad behavior, and $SBB_{i,j}$ stands for its j^{th} dimension. The new position of the i^{th} population member, calculated during the second phase of the proposed MOA, is represented as X_i^{P2} , with its j^{th} dimension indicated by $x_{i,j}^{P2}$. The corresponding objective function value is denoted by F_i^{P2} . The function $\text{rand}(0, 1)$ generates a random number uniformly between 0 and 1, and $\text{rand}(2)$ generates a random integer between 1 and 2, selected uniformly.

3. Exploitation Phase Upbringing

In a number of ways, mothers help their kids develop their academic skills. Parenting enhances the potential for local exploration and exploitation during the MOA period by marginally shifting the population members' placements [13]. To begin simulating the parenting phase, we first assign each population member a new role based on how we predict their personality development using Eq. (14). Based on the description in Eq. (15), if the objective variable result is better within the newest location, the new location is substituted for the previous one of the relevant member.

$$x_{i,j}^{P3} = x_{i,j} + (1 - 2 \cdot \text{rand}(0, 1)) \cdot \frac{ub_j - lb_j}{t}, \quad (14)$$

$$X_i = \begin{cases} X_i^{P3}, & F_i^{P3} \leq F_i; \\ X_i, & \text{else,} \end{cases} \quad (15)$$

Where x_i^{P3} is that j^{th} dimension, F_i^{P3} is the value of its objective function, X_i^{P3} is the new position determined using the third phase of the suggested MOA regarding the i^{th} population member, t is the iteration counter's actual value, the output of the computation function $\text{rand}(0, 1)$ is a random integer between zero and one. Figure 3 shows a flowchart of the steps involved in the proposed MOA.

5. Principle of Partial Shading

Vehicular movement that could block sunlight from reaching PV modules can partially or totally shade them. As a result, solar modules produce more complex output with several peak points. A solar power system that is darkened has multiple local peaks on its PV curve, whereas an array that doesn't have shade has just one peak. Thus, the highest power can only be guaranteed by the global peak and not by any other peak. There are both local and global peaks in Fig. 4. The many consequences of aging could lead to the breakdown of the PV array.

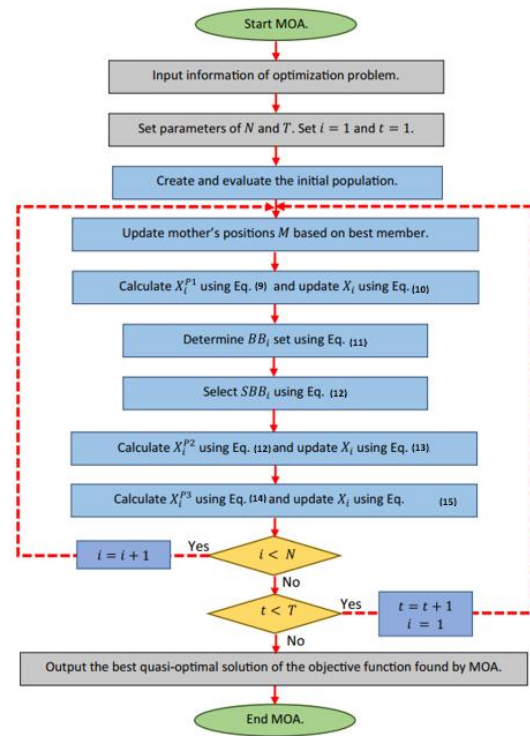


Figure 3. Flowchart of MOA

Designers occasionally overlook the impact of shade, which is simple to overlook. As a result, it's critical to create precise projections of the solar resources that are accessible, accounting for factors like tilt, orientation, and potential solar blockage from structures and trees. To address the issue of partial shadowing, a technological solution that maximizes solar output is also required [16].

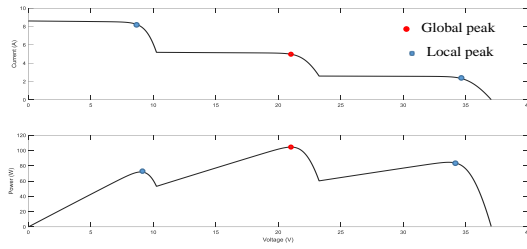


Figure 4. Two types of peaks: global and local

6. Step-Up Converter

As illustrated in Fig. 5, the boost converter is made up of a switch, capacitor, an inductor, source of dc voltage and diode. Resultant voltage from the booster voltage can be computed using the formula below [17]:

$$V_o = (1/(1 - D))V_s \quad (16)$$

Where:

V_s : The boost converter's supply of DC voltage.

V_o : boost converter's output voltage.

D : duty cycle

There is a voltage differential between the input and load resistance R in the DC-DC boost converter [18].

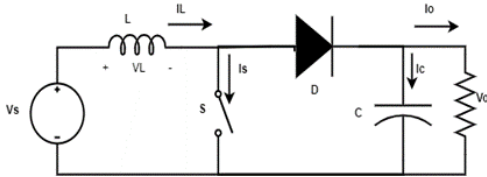


Figure 5. DC-DC boost converter

7. Simulating the electrical schematic

In order to achieve the target output voltage, the circuit design incorporates a string of two PV modules. In this case, the incidence irradiance was 1000W/m² for the first PV module in the string and 800W/m² for the second. The PV module, when coupled with the MPPT, can collect maximum power from the sun and use it in a PSC system. Figure 6 illustrates a PV array linked to a DC-DC boost converter in Simulink, with key features such as maximum power point tracking and partial shading. The output of the DC-DC converter is connected to an 80Ω load. The code for the updated MOA algorithm was developed using S-function builder.

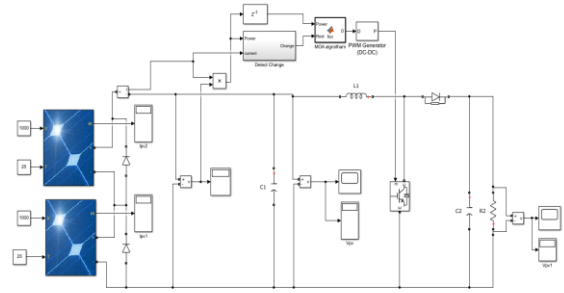


Figure 6. An MPPT-and partially shaded PV array in Simulink

8. Simulation Results and Discussion

The suggested system is designed with a 660W maximum power output. It accomplishes achieved through series-connecting two PV models. The first cell's sun irradiance is 1000 W/m² and the other cell's is 800 W/m² when partially shaded. The output power of the SPV string contains two peaks, one of which represents a one is a worldwide peak, while another is at the regional level, as seen in Fig. 7. This means that the global maximum must be found via the MOA algorithm.

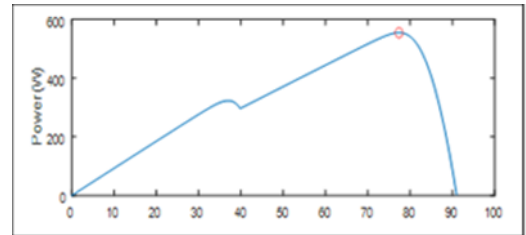


Figure 7. Under partial shade, the P-V characteristic

Figure 8 illustrates the power, voltage, and current output of a DC to DC boosted converter, with the area undergoing transformation being partially shaded using the P&O approach.



Figure 8. Voltage, output current, and power of a DC-DC converter with partial shading using P&O method

Fig. 9 displays the voltage, power, and current output of a DC-DC boosted converter, where the region that is being transformed is partially shaded utilizing the MOA algorithm.

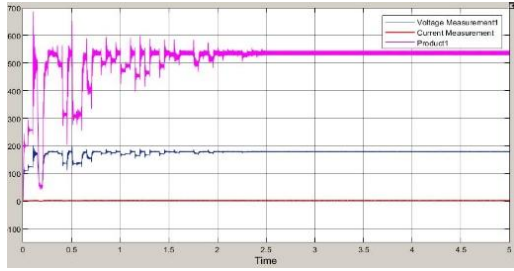


Figure 9. Output voltage, current, and power of a DC-DC converter with partial shading using MOA algorithm

The outcomes for both algorithms (MOA and P&O) are shown in Table 2.

Table 2. obtained results

MPPT	Output power[W]	Output Voltage[v]	Efficiency
P&O	321	219	58.3%
MOA	539	195	98%

The effect of PSC on PV starting efficiency is studied and evaluated under identical conditions using two MPPTs. Based on the Simulink data presented above, the output power collected from the PV string using P&O MPPT is around 321W. However, the output extract power is 539W when using the MOA MPPT. No matter how conditions vary, the MOA algorithm remains accurate, steady, and able to produce a consistent maximum output power with excellent efficiency. Conversely, the P&O MPPT performs poorly under PSC and has a large constant state variation near MPP.

9. Conclusions

The following succinctly describes the primary findings of this study:

- The Mother Optimization Algorithm improves PV efficiency while partially shaded.
- Mother Optimization Algorithm achieved the best results in tracking the Global Maximum Power Point compared to the conventional method.

Conflict of interest

The authors declare no conflicts of interest regarding the current research.

References

1. R. El Idrissi, A. Abbou, M. Mokhlis and M. Salimi, “Adaptive backstepping controller design based MPPT of the single-phase grid connected PV system”, *Int. J. Intell. Eng. Sys.* Vol. 14(3), PP. 282–293, 2021.
2. M. Abdel-Salam, M.T. El-Mohandes and M. El-Ghazaly, “An efficient tracking of MPP in PV systems using a newly-formulated P & O MPPT method under varying irradiation levels”, *J. Electr. Eng. Technol.* Vol. 15(1), pp. 501–513, 2020.
3. A. Harrag and S. Messalti, “PSO-based SMC variable step size P & O MPPT controller for PV systems under fast changing atmospheric conditions”, *Int. J. Number. Model. Electron. Networks, Devices Fields* vol. 32(5), 2019.
4. L. Shang, H. Guo and W. Zhu, “An improved MPPT control strategy based on incremental conductance algorithm”, *Prot. Control Mod. Power Syst.* Vol. 5(1), 2020.
5. M. G. Yahya and M. G. Yahya, “Comparative study of two cases of single-phase HCMLI using IPDPWM technique for standalone PV system,” *International Journal of Nonlinear Analysis and Applications*, vol. 13, no. 1, pp. 2395-2409, doi:10.22075/IJNAA.2022.5940.
6. A. W. Ibrahim, et al., “PV maximum power-point tracking using modified particle swarm optimization under partial shading conditions”, *Chinese Journal of Electrical Engineering*, Vol. 6, No. 4, pp. 106-121, Dec. 2020, doi: 10.23919/CJEE.2020.000035.
7. M. Oulcaid, H. E. Fadil, A. Yahya, et al., “Maximum power point tracking algorithm for photovoltaic systems under partial shaded conditions”, *IFAC-Papers OnLine*, pp. 217-222, 2016, doi: 10.1109/EPEPEMC.2014.6980572.
8. E. Soliman, H. Abd El-Halim, A. Refky, “A proposed an interactive reliable aggregated photovoltaic cell for a longer time solar energy extraction”, *International Journal of Power Electronics and Drive System*, Vol 13, No 1: March 2022 4, doi: 10.11591/ijpeds.
9. A. Siva, V. Rajendran, “A novel auxiliary unit based high gain DC-DC converter for solar PV system with MPPT control”, *International Journal of Power Electronics and Drive System*, Vol 13, No 4:

December 2022, pp. 2386-2395, doi:
10.11591/ijpeds.v13.i4.pp2386-239.

10. K. Boudaraia, H. Mahmoudi and A. Abbou,” MPPT design using artificial neural network and backstepping sliding mode approach for photovoltaic system under various weather conditions”, *Int. J. Intell. Eng. Syst.* Vol. 12(6) pp. 177–186, 2019.
11. González-Longatt, Francisco M. ,”Model of Photovoltaic Module in Matlab”, *i Cibelec 2005*, pp. 1 5,2015.
12. J. Arati, A. Khan, and S. P. Afra., “ Comparison of Half Cut Solar Cells with Standard Solar Cells”, *2019 Advances in Science and Engineering Technology International Conferences (ASET)*. IEEE, 2019.
13. I. Matoušová, P. Trojovský, M. Deghani, *et al.* “Mother optimization algorithm: a new human-based metaheuristic approach for solving engineering optimization”. *Sci Rep* **13**, 10312 (2023). <https://doi.org/10.1038/s41598-023-37537-8>
14. M. G. Yahyaa, M. G. Yahyab, “Comparative study of two cases of single-phase HCMLI using IPDPWM technique for standalone PV system”, *Int. J. Nonlinear Anal. Appl.* **13** (2022) No. 1, pp. 2395-2409.
15. C.C. Ahmed, M. Cherkaoui and M. Mokhlis,” PSO-SMC controller based GMPPT technique for photovoltaic panel under partial shading effect”, *Int. J. Intell. Eng. Syst.* Vol.13(2), pp. 307–316, 2020.
16. H. F. Hashim, M. M. Kareem, W. Kh. Al-Azzawi, A. H. Ali," Improving the performance of photovoltaic module during partial shading using ANN", *International Journal of Power Electronics and Drive System*, vol 12, no 4: December 2021, doi: 10.11591/ijpeds.v12.i4.pp2435-2442.
17. F. Kadir, S.Z. Mohammad Noor, A.H. Faranadia, K.S. Muhammad, " Modeling and simulation of DC to DC boost converter using single phase matrix converter topology ", *International Journal of Power Electronics and Drive System*, vol 11, no 2: June 2020, doi: 10.11591/ijpeds.v11.i2.pp774-784.
18. T.W. Hariyadi and A. Adriansyah, “Comparison of DC-DC converters boost type in optimizing the use of solar panels”, *2nd Int. Conf. Broadband Commun. Wireless Sensors and Powering (BCWSP)*, Yogyakarta, Indonesia, (2020) pp.189–194.